Analytical Methods

Accepted Manuscript

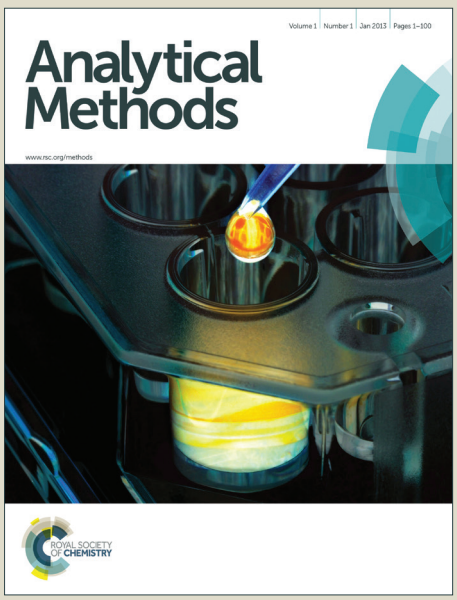

ROYAL SOCIETY OF CHEMISTRY

www.rsc.org/methods

Recent developments in molecular imprinted polymer nanofibers and their applications

Shabi Abbas Zaidi

Department of Chemistry, Kwangwoon University, Wolgye-Dong, Nowon-Gu, Seoul, 139-701, Korea

Correspondence:

E-mail: shabizaidi79@gmail.com

Tel : +82-2-940-8661

Fax: +82-29118584

Keywords: Molecular Imprinted Polymers; Nanofibers; Electrospinning

Abstract

Molecular imprinted polymer (MIP) has been a potential and versatile strategy for analytes detection. The ability to create materials with well-controlled nanofibers is of intense interest for a variety of applications. In recent years, the two fascinating techniques of MIP and nanofibers have been combined to facilitate and achieve greater benefits through pre-synthesized MIP nanoparticles or microspheres encapsulation in nanofibers via electrospinning or direct reaction conditions. On the other hand, there are few excellent reports where MIP reaction constituents were dissolved into uniform and homogeneous electrospinning solutions to achieve MIP electrospun nanofibers. This article is the very first review reporting on the development of MIP nanofibers preparation and their applications for the determination of several valuable compounds in various areas.

Introduction

Molecular imprinted polymers (MIPs) are cross-linked polymers that exhibit specific binding sites for the template molecule. MIPs are obtained from Molecular imprinting technique (MIT) which is considered an effective, versatile and robust approach where any template molecule (analyte of interest) is introduced in a mixture of monomer and cross-linker dissolved in a solvent resulting into three-dimensional polymer matrix molecular imprinted polymer (MIP). Subsequent removal of the template from as–prepared polymer, the permanent cavities of the original template is formed which are capable to rebind selectively to the template molecules. The obtained polymer, referred as molecular imprinted polymer (MIP), demonstrates high stability and robustness in harsh synthesis and analysis environment. G. Wulff (1972)[1] propounded the MIP preparation method based on covalent bonding, whereas K. Mosbach (Arshady 1981)[2] developed MIP involving non-covalent bindings. Most MIPs today are prepared by employing non-covalent approach due to its fast adsorption kinetics and easy preparation protocols compared to covalent approach. The morphology of MIP can be tailored by carefully optimizing the experimental parameters and amount of reaction constituents. Finally, the obtained imprinted cavities are capable of rebinding the target molecule with a high specificity, sometimes comparable to that of antibodies.

Since last two decades, extensive research efforts have been devoted for the fabrication and development of the MIPs. Due to their high selectivity and stability, MIPs have been applied for numerous applications such as chromatographic separation,[3,4,5,6,7] recognition for peptides and biomolecules,[8] capturing of hazardous radioactive waste,[9] drug delivery,[10,11] solid phase extraction,[12] and recognition element for electrochemical and biosensors.[13,14,15] Although, the utilization of MIP as recognition elements in electrochemical sensors have shown promising results, however, MIPs fabricated by the conventional methods pose few drawbacks including slow mass transfer rate and low adsorption capacity. These obstacles have fueled research to utilize materials possessing high surface area such as nanomaterials.[16, 17, 18] Among many nanomaterials, nanofibers have been increasingly utilized owing to few intriguing features such as nanosize offering high surface area, flexibility in surface functionalities, and superior mechanical performance (e.g. stiffness and tensile strength). Furthermore, the biocompatible matric polymer precursor solution leads to the formation of biocompatible nanofibers which can

potentially be utilized in drug delivery and related applications. A great deal of discussion on the current and future perspective on electrospinning functional nanofibers has been provided in an excellent review elsewhere.[19]

Several research works have been carried out by combining the amazing properties of MIPs and nanofibers to obtain molecular imprinted polymer nanofibers (MIP-NFs) which possess outstanding qualities such as more reliable and sustained release of imprinted drug in MIPs compared to drug scaffold which can lead to burst release and less effective life time (more complex co-axial technique is used to prevent burst release). In addition, MIP-NFs possess high loading and reloading possibility, easier release of drug due to non-covalent bonding between imprinted molecule and polymer compared to some scaffolds utilizing covalent drug bonding and suitable in any harsh environmental conditions (i.e. pH or temperature) until they are synthesized to be stimuli responsive, greater surface area and loading capacity for more MIP drug loading, high mechanical strength, and biocompatibility offered by nanofibers.

Based on the published reports, it has been deduced that MIP-NFs is one of the fascinating materials used for diverse applications including drug delivery, protein detection, and other smaller molecules detection. However, it is worth noticing that there are not huge reports on MIP-NFs in any field despite their efficient and versatile characteristics. Nevertheless, it is necessary to summarize the work which has been performed in this area to understand the merits and demerits of the material so that it could attract due attention. As a result, this mini review represents a detailed discussion on literature published in recent years comprising MIP-NFs.

Synthesis methods and reaction parameters of NFs

There are many processing techniques such as drawing, template synthesis, phase separation, self-assembly, electrospinning, etc. have been used to prepare polymer nanofibers in recent years.[20]

Of these, electrospinning is the most widely studied technique allowing the creation of polymer fibers with diameters in the range of a few tens of nanometers to a several micrometers (usually between 50 and 500 nm) through the action of an external electric field imposed on a polymer solution or melt. There are two electrospinning processes, vertical and horizontal. An

electrospinning system consists of three major components: a high DC voltage supplier, a capillary tube with a pipette or needle of small diameter (i.e. spinneret), and a grounded metal collecting screen or plate. Most of the polymers are dissolved in some solvents before electrospinning. The polymer solution which is held by surface tension with appropriate experimental conditions is filled into syringe and a high voltage is applied on spinneret. When the electric field applied reaches a critical value, the repulsive electrical forces overcome the surface tension forces. Eventually, a charged jet of the solution is ejected from the tip of the Taylor cone and an unstable and a rapid whipping of the jet occurs in the space between the capillary tip and a collector of opposite polarity followed by evaporation of the solvent, leaving a polymer behind.[21,22] A schematic of electrospinning technique has been shown in Figure 1.

The size of electrospun NFs can be customized easily by varying the experimental conditions of electrospinning such as (a) the solution properties including viscosity, elasticity, conductivity, and surface tension, (b) governing variables such as hydrostatic pressure in the capillary tube, electric potential at the capillary tip, and the gap (distance between the tip and the collecting screen), and (c) ambient parameters such as solution temperature, humidity, and air velocity in the electrospinning chamber and seems to exhibit the most promising results owing to simplicity and versatility of technique.[20,23]

Synthesis methods of MIP-NFs

There are usually two methods of preparation of MIP-NFs. In the first approach, MIP is synthesized followed by entrapping of MIP in electrospun polymer nanofibers, thus creating a nonwoven mat of sensing sites with a high surface area and accessibility. In the second approach, the imprinted molecule is directly introduced in the polymer solution containing functional monomer and polymer matrix which is then electrospun to achieve MIP-NFs.

The first approach is widely used as it provides more flexibility for the preparation of various types of tailored MIP which can be incorporated in the polymer solution in electrospinning despite that it may prove to be tedious. On the contrary, second approach is simple and less time consuming, however, size control of imprint cavities may be cumbersome. Nevertheless, there have been reports on both types of approaches.

Applications of MIP-NFs

Due to its high efficiency, simplicity, and high affinity between membrane and target analytes, the membrane separation technique has been regarded a potential separation method. Inspiring from excellent features of membrane separation technique and utilizing the unique qualities of MIPs and nanofibers, numerous reports have been published on the synthesis of Molecular imprinted nanofibers membrane.[24] The following section will deal with the applications of Molecular imprinted nanofibers membrane approaches.

Yoshimatsu et al.[25] synthesized propranolol imprinted nanoparticles and encapsulated them into poly(ethylene terephthalate), PET, nanofibers through electrospinning. The resulting composite membranes were characterized by scanning electron microscopy (SEM) and radio ligand binding analysis. Finally, solid phase extraction (SPE) of aqueous propranolol from water using the nanofiber membrane was carried out, and selective recovery of propranolol was verified by quantitative HPLC–MS/MS analysis. It was observed that small MIP nanoparticles were easily encapsulated in PET nanofibers compared to large size MIP nanoparticles. The proposed MIP nanofiber membrane was selective in the presence of other structural analogues such as atenolol, metopronolol (+)-tartrate, timolol maleate, pindolol and acebutolol hydrochloride. It was also successfully applied in the detection of propranolol in spiked tap water.

A simultaneous enhancement in permselectivity and flux (throughput) was achieved for a derivative of optically pure glutamic acid, such as N-α-benzyloxycarbonyl-d-glutamic acid (Z-d-Glu) or N-α-benzyloxycarbonyl-l-glutamic acid (Z-l-Glu) with 30 wt % cellulose acetate (CA) in N,N-Dimethylformamide (DMF) by applying an electrospray deposition technique. The control molecularly imprinted membranes were also prepared for comparison study. The molecularly imprinted nanofiber membranes were characterized and compared in terms of adsorption selectivity, affinity constant, permselectivity, and flux. The results obtained in the present study revealed that molecularly imprinted nanofiber membranes were about two orders of magnitude higher and also provided permselectivity than the usual molecularly imprinted membranes.[26]

Buttiker et al.[27] developed MIP nanofibers membrane for cinchonidine, an alkaloid having antimalarial activity. Firstly, cinchonidine MIP microspheres of 4-5 μm were synthesized with

methacrylic acid (MAA) and divinylbenzene (DVB). The as-prepared MIP microspheres were immobilized by incorporating them into membranes of polyacrylonitrile (PAN) nanofibers with different diameter through electrospinning. The morphology of MIP nanofiber membranes were studied by SEM and the high affinity of the composite membrane for cinchonidine enabled to localize the cinchonidine binding sites by Raman spectroscopy and Fourier transform infrared spectroscopy (FTIR) techniques.

In order to fabricate Rhodamine B (RhB) imprinted electrospun nanofiber membrane, Liu et al.[28] synthesized RhB imprinted microspheres by precipitation polymerization. Later, these microspheres were incorporated in membrane produced via electrospinning technique with polyethylene terephthalate (PET) as the matrix polymer. The as-synthesized MIP microspheres and MIP nanofiber membrane were characterized by SEM. Under optimized conditions, the linear range of 0.01- 20 $\mu mol \cdot L^{-1}$ and detection limit for RhB was found to be 2 $nmol \cdot L^{-1}$. The results demonstrated that the imprinted polymer electrospun nanofiber membrane exhibited higher affinity for Rh B compared to non-molecularly imprinted polymer membranes (NIMs) and molecularly imprinted particles (MIPs).

Yoshikawa and co-workers prepared and demonstrated the comparison results for the fabrication of molecularly imprinted membranes (MIPMs) and molecularly imprinted nanofiber membranes (MINFMs) from polysulfone with aldehyde and N-α-benzyloxycarbonyl-d-glutamic acid (Z-d-Glu) N-α-benzyloxycarbonyl-l-glutamic acid (Z-l-Glu) as a print molecule using molecular imprinting and an electrospray deposition techniques, respectively. The as-fabricated two types of molecularly imprinted membranes showed good chiral separation by membrane transport. However, the MINFMs offered one to two orders of magnitude higher flux than those of usual MIPMs without depression of permselectivity. It was concluded that inclusion of nanofiber enhanced the activity of MINFMs.[29]

A Propranolol selective molecular imprinted polymer composite electrospun nanofiber membrane was developed. The propranolol imprinted beads were prepared by oil/water emulsion polymerization using MAA and DVB followed by their entrapment in Eudragit-RS100 nanofiber membrane via electrospinning. For comparison studies, the non-imprinted polymers (NIPs) were

prepared using the same method as the MIP but without the addition of the Propranolol template during polymerization. The morphology and diameter of the MIP beads, NIP beads, MIPs and NIPs composite Eudragit-RS100 fiber membranes were determined using a SEM and chemical composition of nanofiber membranes were confirmed. The MIP composite Eudragit-RS100 nanofiber membrane exhibited high propranolol loading and reloading than NIP nanofiber membrane and showed higher selectivity to propranolol than to other β-blockers.[30]

Li et al.[31] introduced an excellent strategy for the fabrication of glycoprotein imprinting nanofiber membrane by utilizing magnetic Fe3O4@Au multifunctional nanofibers. Firstly, Fe3O4@Au nanoparticles were synthesized and polymer nanofibers were functionalized by introducing boronic acid and polymerizable double bonds with Fe3O4@Au nanoparticles as the substrate. The template glycoprotein (horseradish peroxidase) was directly covalently grafted on the surface of the functional NFs and then polymerized via radical induced graft copolymerization as shown in figure 2. The control non-imprinted nanofibers (NIPs) were prepared and washed in the same way but without addition of the template. The successful stepwise synthesis during experiments was confirmed by FTIR and Thermogravimetric analysis (TGA) analysis. The morphological structures of Fe_3O_4@Au multifunctional nanofibers and MIPs were also investigated by Transmission electron microscopy (TEM) which showed the average diameter of about 80 nm to 160 nm, respectively, which indicates that multifunctional nanofibers were successfully embedded with polymers. The MIP performed well in adsorption studies and electrochemical experiments. The MIP gave good linearity in the range of low concentrations from 0.01 to 0.30 mg mL^{-1} with a LOD of 0.005 mg mL^{-1} and exhibited good regeneration capacity and reproducibility.

Wu et al.[32] demonstrated the dual-imprinted polymer nanofiber membrane (nano-MIMs) for selective detection of biphenyl A (BPA) and tebuconazole (TBZ) in vegetable and juice samples by membrane-based molecularly imprinted through solid-phase extraction (m-MISPE) and HPLC. Initially, BPA and TBZ imprinted nanoparticles (NPs) were prepared separately. Additionally, NIPs were also prepared with same protocol but without template. The Nano-MIMs were prepared by encapsulating different MIP-NPs or corresponding NIP-NPs into polyvinyl alcohol (PVA) nanofibers through electrospinning as shown in Table 1 and their

corresponding SEM images have been assembled in Figure 3. As shown in table 1, nanofibers membrane containing MIP NPs and NIP NPs were prepared. Moreover, nanofibers containing single MIP NPs, NIPs as well as nanofibers containing mixed template MIPs and NIPs were also prepared for comparison. It is clear from figure 3 that as-fabricated MIP NPs were distributed evenly along the nanofibers. The diameter of composite nanofibers was in the range of 0.4-1μm. Finally, the nano-MIMs gave higher than 70.33% recoveries with less than 9.57% of relative standard deviations (RSDs) of BPA and TBZ with m-MISPE and HPLC from different samples which was better than conventional SPE based on C18/SCX.

Yoshikawa group studied the fabrication of molecular imprinted nanofiber membrane (delocalization) and core-shell molecular imprinted nanofiber membrane by usual single spinneret and a co-axial, two capillary spinneret electrospray deposition for L or D-phenylalanine (L or D-Phe) with chitosan (CS). The as-synthesized membranes were characterized with SEM and their performances were compared with adsorption experiments. It was observed that core-shell nanofiber membrane exhibited higher membrane transport due to localized (on the surface) imprinting cavities over nanofiber than to usual nanofiber membrane where imprinted cavities were embedded inside nanofiber.[33]

In one report, molecularly imprinted nanofiber membranes (nMIM) were fabricated by encapsulating BPA-imprinted polymeric nanoparticles (MIPs) into biocompatible polyvinyl alcohol (PVA) nanofibers using electrospinning. For comparison, nMIM, nNIM (non-imprinted nanofiber membrane), PVA membrane with MIP incorporation were also prepared. Then, MIM was used to enhance the degradation of BP by P. aeruginosa which could be attached and immobilized on the biocompatible MIM. The increased level and the amounts of immobilized bacteria on the membranes were strongly correlated to BPA biodegradation rate and the MIM could continuously enhance the degradation of trace BPA (2μg/L) in waste water during a 10-day experiment. The study showed that the Langmuir equation fits the adsorption isotherms better than the Freundlich equation.[34]

Javanbakht group prepared Sol-gel based acesulfame (ACF) imprinted polymer nanofiber by electrospinning on the surface of a stainless steel bar which was connected for on-line selective

solid phase microextraction (SPME) with high performance liquid chromatography (HPLC). In this method, 3-(triethoxysilyl)-propylamine (TMSPA) was selected as a precursor and Nylon 6 was also added as a backbone and support for the precursor in which sol could grow during the sol-gel process and make the solution electrospinable. The HPLC results showed that the linearity for the ACF in beverage sample was in the range of 0.78–100.5 ng mL^{-1} and LOD and limit of quantification (LOQ) were 0.23 and 0.78 ng mL^{-1}, respectively.[35]

In an simple and direct approach, Chronakis et al.[36] developed a 2,4-dichlorophenoxyacetic acid (2,4-D) imprinted polymer electrospun nanofibers. They utilized a solution mixture of poly(ethylene terephthalate) (PET) as matrix polymer and polyallylamine as functional monomer. The solution was filled in a syringe and continuous well-defined nanofibers were collected over aluminum foil kept at a distance of 20 cm and worked as counter electrode. The template was removed and characterized with SEM, FT-IR techniques and radio ligand binding analysis. The 2,4-D imprinted nanofibers displayed favorable binding characteristics in aqueous solution.

In another interesting approach, Chronakis et al.[37] prepared two different molecules nanofibers. Theophylline and 17β-estradiol imprinted nanoparticles were synthesized and encapsulated into 10% by weight of Poly (ethylene terephthalate) (PET) nanofibers via electrospinning. The SEM characterization showed that MIP NPs were uniformly distributed in PET nanofibers and the composite nanofibers had an average diameter of 150-300 nm, depending on the content of MIP nanoparticles. It is clear from the results obtained via radio ligand binding analysis that the imprinted nanofiber bound more than the non-imprinted nanofiber as shown in Figure 4.

In one approach referred as ‘‘rapidly mixed reaction’’, a self-assembly strategy to prepare 4-hydroxybenzoic acid (4-HA) surface imprinted polyaniline (PANI) nanofiber was discussed by Cao and co-workers. The nanofibers were synthesized by dissolving aniline and 4-HA in highly acidic distilled water (pH~ 2.0) in the presence of initiator ammonium peroxydisulfate (APS) and polymerization was initiated for 24 h at room temperature. The synthesized nanofibers were washed and dried. The nanofibers were characterized by SEM and TEM which verified the formation of PANI NFs with an average diameter range from 50 nm to 70 nm and several

micrometers in length. The steady-state binding assay showed that MIP nanofibers have large adsorption capacity and fast uptake kinetics for target species compared to NIP nanofibers.[38]

Yoshimatsu and co-workers demonstrated another fascinating strategy to introduce signal transduction ability into molecularly imprinted nanofibers via scintillation material in electrospinning technique as shown in Figure 5. Firstly, an organic scintillator, 9,10-diphenylanthracene (DPA) was easily electrospun in polystyrene (PS) nanofibers to obtain DPA-doped nanofibers. Then, propranolol-MIP nanoparticles were prepared and these are entrapped in DPA-doped nanofibers. The as-fabricated nanofibers were characterized by SEM and radio ligand binding analysis. The SEM analysis showed fabrication of well-defined morphology and that the diameter of the nanofibers containing nanoparticles was about 250–500 nm which was slightly increased due to the encapsulation of the nanoparticles. The labeling results also supported the evidence that the incorporation of DPA enhanced the signal transduction ability of nanofibers compared to the nanofibers synthesized without DPA.[39]

To prepare a fluorescent amino acid derivative dansyl L-phenylalanine (dansyl-L-Phe) imprinted biosensor, dansyl-L-Phe MIP nanoparticles were synthesized via precipitation polymerization and particles with a diameter of 400 nm were obtained, as determined by dynamic light scattering. The NIP nanoparticles were also obtained with similar protocol but without template. Later, the as-prepared MIP and NIP nanoparticles were included in poly(vinyl alcohol) (PVA) nanofibers by electrospinning. The morphology of nanofibers was characterized by atomic force microscopy and optical microscopy. The binding of the target molecule and other related molecules to the fibers was characterized by fluorescence microscopy. The binding analysis of dansyl-L-Phe to MIP-PVA as a function of concentration represents a Langmuir binding isotherm with KD value of 21± 5 μM and it also showed selective binding for MIP-PVA nanofibers compared to NIP-PVA nanofibers.[40]

Xiuling et al.[41] fabricated Naringin (NG) imprinted nanofibers in the presence of β-CD as a functional monomer and polyvinylbutyral (PVB) as matrix polymer through electrospinning. Then, resultant NG nanofibers were immersed into Hexamethylene diisocyanate (HMDI, cross-

linker) at 30 ℃ for 24 h and then, the template molecules were removed. The as-prepared nanofibers were successfully characterized by SEM, XRD, and FTIR techniques. The binding experiments results provided excellent imprinting effect and selectivity for imprinted nanofibers compared to non-imprinted nanofibers and traditional MIPs.

In one report, 1,3-dinitrobenzene (DNB) imprinted PANI NFs were synthesized. In order to fabricate, PANI NFs were synthesized followed by their functionalization to generate vinyl moieties which could be easily attached on MIP surface. These functionalized PANI NFs were mixed into appropriate amount of monomer (acrylamide, AA), cross-linker (Ethylene glycol dimethacrylate, EDMA) and initiator (azobisisobutyronitrile, AIBN). The thermal polymerization was carried out to achieve MIP nanofibers. Traditional MIP was also prepared for comparison. The as-prepared PANI MIP nanofibers were characterized by SEM, FTIR and UV-Vis spectroscopy. The electrochemical behavior was investigated by CV (cyclic voltammetry) and EIS (electrochemical impedance spectroscopy). The sensor offered a linear response of DNB concentration between 2.20×10^{-8} and 3.08×10^{-6} M with LOD of 7.33×10^{-9} M. The excellent selectivity, stability and reproducibility was achieved for DNB sensor.[42]

Kim and Chang [43] developed an estrone imprinted polyimide nanofiber through electrospinning. Firstly, estrone made complex with pre-synthesized polyimide, an aromatic diamine (i.e. functional monomer). The template-monomer complex was electrospun in the presence of poly(amic) acid to obtain estrone imprinted polyimide nanofiber. The structural morphology and size of as-fabricated nanofibers were optimized by changing the solution concentration and the applied voltage, keeping other electrospinning parameters such as the separation distance, flow rate, and the diameter of needle, constant. Under optimized conditions of 20% by wt of poly(amic) acid and 20KV applied voltage, nanofibers with an average diameter of 150 nm were collected as a fibrous mats. The well-defined morphology of nanofibers was obtained as conformed by SEM analysis. In binding experiments, the estrone imprinted nanofibers exhibited selectivity and fast binding kinetic by achieving 80% equilibrium in just 10 min which was attributed to a large surface area of the imprinted nanofibers.

Kim et al.[44] introduced another captivating strategy for theophylline imprinted organogel nanofiber synthesis. This was synthesized by using two pre-synthesized compounds: one is heterobifunctional organogelator possessing two polymerizable groups and second is functional monomer with similar structure to organogelator. The functional monomer-template complex was incorporated in heterobifunctional organogelator with a crosslinker (DVB) and initiators to achieve stable imprinted organogel nanofibers. The schematic representation of preparation, SEM, and the kinetic binding profile of the MIPG and NIPG nanofibers for the theophylline are shown in Figure 6. As seen in figure 6, dried organogel formed entangled fibers with diameters ranging from 80 nm to 100 nm, whereas, MIPG nanofibers showed much more distinct fiber structures with the same or slightly increased diameters compared with the dried gel indicating a successful polymerization in organogel. The Differential scanning calorimetry (DSC) and FTIR analysis were also performed to support the successful synthesis and polymerization in organogel. Furthermore, it can also be perceived from figure 6 that MIP organogel nanofibers showed a specific binding ability, increased binding and a fast kinetic binding profile toward template as compared to NIP organogel nanofibers.

Piachem et al.[45] reported on the quercetin-imprinted polymer coating bacterial cellulose nanofiber (QIP-BC) in a simple approach. The BC was produced from *Acetobacter Xylinum* and then mixed in the prepolymerization mixture containing quercetin, 4-vinylpyridine (4-VP), EDMA, and AIBN in excess of methanol for 48 h. Subsequently, thermal-induced polymerization was initiated at 60°C for 72 h. The control polymer was obtained without template. The polymerization process took place in a dilute solution and therefore, the imprinted polymer could be generated on both BC nanofibers and nanospheres in the solution. The binding analysis showed that QIP-BC provided three-fold higher recognition ability for quercetin than quercetin imprinted nanospheres.

In a very interesting approach for the desulfurization of fuels presented by Ogunlaja et al.[46], benzothiophene sulfone, dibenzothiophene sulfone and 4,6-dimethyldibenzothiophene sulfone were used as templates for the preparation of imprinted polymers glutaraldehyde cross-linked chitosan microspheres. It was followed by incorporating all MIP microspheres in an appropriate amount of styrene and nanofibers were obtained by electrospinning. The template molecules

within the nanofibers matrix were removed via soxhlet extraction using a mixture of methanol and acetonitrile (1:1). The detailed characterization of materials was carried out by SEM, FTIR and TGA. Furthermore, swelling studies were also used to investigate the behavior of microspheres and nanofibers. The adsorption kinetic studies clearly indicated that the imprinted nanofibers outperformed the MIP microspheres and sulfone compounds exhibited well fitted Freundlich isotherm and pseudo-first-order model. The application of the nanofibers to oxidized hydro-treated fuel under continuous flow adsorption system at 1 mL/h indicated that 84% of sulfur was adsorbed, with adsorption capacity of 2.2 ± 0.2 mg/g.

Ruggieri et al.[47] demonstrated about atrazine imprinted polystyrene- based molecularly imprinted polymer nanofibers through the electrospinning technique and the structures of the MIPs and NIPs were visualized by SEM. It was found by batch adsorption experiments for atrazine that the Freundlich isotherm model explains better the experimental data than the Langmuir isotherm model. The MIP nanofibers showed excellent results compared to NIP membrane. Furthermore, the as-synthesized membrane showed good efficiency at higher analyte concentrations compared to commercial stationary phases which performed well at low pesticide concentrations in solid phase extraction (SPE).

The Li group[48] introduced another related approach for vinyl functionalized magnetic nanofibers for Lysine (protein) imprinting. In the first step, Fe_3O_4 NPs were doped in the MIPs because they have unique magnetic properties that enable them to be handled by magnetic field and facilitate separation and purification of nanomaterials in the synthesis process. Secondly, p-amino-thiophenol (PATP) capped Fe_3O_4 @Au NPs were formed in order to introduce aniline groups (polyaniline, PA) for copolymerization with aniline. Thirdly, a vinyl group was introduced onto the Fe_3O_4@Au@PA NF surface with amide reaction of acryloyl chloride which produced a fast response and high-yield. The as-synthesized MIP magnetic nanofibers were investigated by TEM and FTIR. TEM showed that MIP is attached over substrate and a rigid linear structure compared to traditional NFs or nanowires which usually exhibited toughness and curves in MIP technology was clearly visible. Furthermore, the FTIR spectra were taken to characterize the composition of material. The adsorption study was shown to obey Freundlich isotherm and the pseudo-first-order model and the calculated values were in better agreement with the experimental values.

Challenges in MIP nanofiber

Despite many superior features, there are few challenges encountered for the fabrication of MIP nanofibers during electrospinning and simple thermal polymerization techniques. The first major challenge is to effectively synthesize nano-controlled size of MIP which could be entrapped easily into nanofibers mats during electrospinning. The low throughput or production rate is another challenge during nanofibers synthesis which can be overcome by a two-layer electrospinning system to some extent; however, more reliable method is in demand. Controlling the electrospinning parameters is another very crucial point in order to electrospun the well-defined nanofibres mat. Among many parameters, the environmental humidity which affects the solution viscosity is highly critical for good shape of nanofibers. In addition, one of the critical limitations of electrospinning is the formation of small pore size and lack of proper cellular infiltration inside the fibers. Some improvements have been reported in this direction but a lot more attention to achieve appropriate pore size control connecting throughout nanofibres length is required. Sometimes, poor mechanical strength of MIP nanofibers fails to impress the scientists working in this field. Hence, robust matrix polymer with good biocompatibility is required.

During incorporation of MIP into nanofibers, the complete removal of imprinted molecules from nanofibers poses another hurdle; which can be avoided by applying surface imprinting. There are few more limitations of electrospinning which affect its wide utility for the fabrication of MIP-NFs such that it could not fabricate an effective dense membrane needed for diffusion-based separation procedures in reverse osmosis and nanofiltration. The limitations of electrospinning technique such as pore size, electrical conductivity, mechanical strength, hydrophobicity which might be beneficial for practical implementation in MIP based NFs can be achieved by post-treatment of electrospun nanofibers membranes by using thermal or chemical treatment. Thus, more robust, controlled, and improved electrospinning techniques may be needed in this direction.

Conclusion and Future perspective

This mini review is the first comprehensive report focusing the development and application of MIP nanofibers. The preparation of MIP nanofiber approach is the combination of two fascinating materials, MIP and nanomaterials. In this review, we discussed all the reports related

to this topic and concluded that this technique is very attracting. However, despite the many excellent and unique advantages, there has been not much research done in this area.

It can be expected by viewing the trend for last 2-3 years that MIP nanofibers approach is receiving increased attention. Particularly, this can be a convenient and potential strategy in drug delivery as it offers sustained release of drugs compared to some polymer scaffold which can lead to burst release and less effective life, high loading capacity with easy release as drug binds non-covalently and biocompatibility. It is also worth noticing that this approach will be very useful in other critical areas such as radiowaste removal, demetallation in fuels, and food industry. In addition, MIP nanofibers can effectively be employed in the fabrication of smart filters to remove hazardous pollution substances and more robust synthetic biomimetic receptors such as antibodies. Moreover, it is known that signal transduction ability of MIP is poor, thus some more good and simple strategy to increase signal transduction ability for the fabrication of MIP nanofibers is also on the card.

Acknowledgement

This research is supported by Kwangwoon University in 2015.

References

1. G. Wulff, and A. Sarhan, *Angew Chem*., 1972, 84, 364- 364.
2. R. Arshady, and K. Mosbach, *Macromol Chem*., 1981, 182, 687- 692.
3. S.A. Zaidi, and W.J. Cheong, *J. Chromatogr. A* 2009, 1216, 2947-2952.
4. S.A. Zaidi, *Electrophoresis* 2013, 34, 1375-1382.
5. S.A. Zaidi, S.M. Lee, and W.J. Cheong, *J. Chromatogr. A* 2011, 1218, 1291-1299.
6. M.R. Halhalli, E. Schillinger, C.S.A. Aureliano, and B. Sellergren, *Chem. Mater.*, 2012, 24, 2909–2919.
7. H. Lu and G. Chen, *Anal. Methods*, 2011, 3, 488-508.
8. D.S. Janiak, and P. Kofinas, *Anal Bioanal Chem*., 2007, 38, 399–404.
9. A. Bhaskarapillai, N. Sevilimedu, and B. Sellergren, *Ind. Eng. Chem. Res.,* 2009, 48, 3730- 3737.
10. S.A. Zaidi, *Drug Delivery* 2014, (doi:10.3109/10717544.2014.970297
11. F. Puoci, G. Cirillo, M. Curcio, O.I. Parisi, F. Iemma, N. Picci, *Expert Opin Drug Deliv.,* 2011, 8, 1379-93.
12. B. Sellergren, *Trends Anal. Chem.,* 1999, 18, 164–174.
13. D. Zhang, D. Yu, W. Zhao, Q. Yang, H. Kajiura, Y. Li, T. Zhou, and G. Shi, *Analyst*, 2012,**137**, 2629-2636.
14. X. Wang, J. Dong, H. Ming, and S. Ai, *Analyst*, 2013,138, 1219-1225.
15. Y. Peng, Z. Wu, and Zhigang Liu, *Anal. Methods*, 2014, 6, 5673-5681.
16. L. Ying, L. Xin, C. Dong, J. Qi, and X. Han, *Carbon* 2010, 48, 3427-3433.
17. S.A. Zaidi, *Int. J. Electrochem. Sci*., 2013, 8, 11337-11355.
18. W.R. Huang, Y.L. Chen, C.Y. Lee, and H.-T. Chiu, *RSC Adv.,* 2014, 4, 62393-62398.
19. M.T. Hunley, and T. E Long, *Polym Int.,* 2008, 57, 385–389.
20. Z.-M. Huang, Y.-Z. Zhang, M. Kotakic, S. Ramakrishna, *Compos. Sci. Technol.,* 2003, 63, 2223–2253.
21. N. Bhardwaj, and S.C. Kundu, *Biotechnol. Adv.,* 2010, 28, 325–347.
22. R. Vasita, and D.S Katti, *Int. J. Nanomedicine* 2006, 1, 15–30.
23. J. Doshi, and D.H. Reneker, 1995, 35, 151– 160.

24. M. Yoshikawa, A. Tanioka, and H. Matsumoto, *Curr. Opin. Chem. Engg.,* 2011, 1, 18–26.
25. K. Yoshimatsu, L.Ye, J. Lindberg, I.S. Chronakis, *Biosens. Bioelectron.,* 2008, 23, 1208–1215.
26. Y. Sueyoshi, C. Fukushima, M. Yoshikawa, *J. Membr. Sci.,* 2010, 357, 90–97.
27. R. Büttiker, J. Ebert, C. Hinderling, and C. Adlhart, *CHIMIA,* 2011, *65*, 182-186.
28. H. Liu, X. Lei, Y. Zhai, and L. Li, *Adv. Chem. Engg. Sci.,* 2012, 2, 266-274.
29. Y. Sueyoshi, A. Utsunomiya, M. Yoshikawa, G.P. Robertson, and M.D. Guiver, *J. Membr. Sci.,* 2012, 401-402, 89–96.
30. P. Tonglairoum, W. Chaijaroenluk, T. Rojanarata, T. Ngawhirunpat, P. Akkaramongkolporn, and P. Opanasopit, *AAPS Pharm. Sci. Tech.*, 2013, 14, 838-846.
31. Y. Li, M. Hong, M., Q. Bin, Z. Lin, Z. Cai, and G. Chen, *J. Mater. Chem. B,* 2013, 1, 1044–1051.
32. Y.-T. Wu, Y.H. Zhang, M. Zhang, F. Liu, Y.-C. Wan, Z. Huang, Q. Zhou, Y. Shi, and B. Lu, *Food Chemistry,* 2014, 164, 527–535.
33. J. Isezaki, and M. Yoshikawa, *J. Membr. Sep. Technol.,* 2014, *3,* 119-126.
34. F. Liu, Q. Liu, Y. Zhang, Y. Liu, Y. Wan, K. Gao, Y. Huang, W. Xia, H. Wang, Y. Shi, Z. Huang, and B. Lu, *Chem. Engg. J.,* 2015, 62, 989–998.
35. M. M. Moein, M. Javanbakht, M. Karimi, and B.A. Adergani, *Talanta* 2015, 134, 340–347.
36. I.S. Chronakis, B. Milosevic, A. Frenot, and L. Ye, *Macromolecules* 2006, *39,* 357-36.
37. I.S. Chronakis, A. Jakob, B. Hagstrom, and L. Ye, *Langmuir* 2006, *22,* 8960-8965.
38. F. Cao, J. Liao, K. Yang, P. Bai , Q. Wei, and C. Zhao, *Anal. Letters,* 2010, 43, 2790–2797.
39. K. Yoshimatsu, L. Ye, P. Stenlund, and I.S. Chronakis, *Chem. Commun.,* 2008, 17, 2022–2024.
40. S. Piperno, B.T.S. Bui, K. Haupt, and L.A. Gheber, *Langmuir* 2011, 27, 1547–1550.
41. X. Ma, Z. Chen, X. Chen, R. Chen, and X. Zheng, *Chin. J. Chem.* 2011, *29*, 1753-1758.
42. Y. Liang, L. Gu, X. Liu, Q. Yang, H. Kajiura, Y. Li, T. Zhou, and G. Shi, *Chem. Eur. J.,* 2011, 17, 5989 – 5997.
43. W.J. Kim, and J.Y. Chang, *Mater. Letters* 2011, 65, 1388–1391.
44. W.J. Kim, B.M. Jung, S.H. Kang, and J.Y. Chang, *Soft Matter,* 2011, 7, 4160–4162.

45. T. Piacham, C. Isarankura-Na-Ayudhya, V. Prachayasittikul, *Chem. Pap.,* 2014, 68, 838–841.

46. A.S. Ogunlaja, M.J. Coombes, N. Torto, and Z.R. Tshentu, *React. Funct. Polym.,* 81 (2014) 61–76

47. F. Ruggieri, A. A. D'Archivio. D. Di Camillo, L. Lozzi, M. A. Maggi, R. Mercorio, and S. Santucci, *J. Sep. Sci.* 2015, *38*, 1402–1410.

48. Y. Li, Q. Bin, Z. Lin, Y. Chen, H. Yang, Z. Cai , and G. Chen, *Chem. Commun.,* 2015, 51, 202-205.

Figure Captions

Figure 1. Schematic diagram of set up of electrospinning apparatus (a) typical vertical set up and (b) horizontal set up of electrospinning apparatus (21) Reproduced with permission from Elsevier publishers.

Figure 2. Synthesis route of Fe_3O_4@Au@PA–APBA–AA MIPs (PATP = p-aminothiophenol; APBA = 3-aminophenylboronic acid; APS = ammonium persulfate; MAA = methacrylic acid; AAm = acrylamide; MBA = N,N-methylenebisacrylamide; TEMED = N,N,N,N-tetramethylethylenediamine) (31) Reproduced with permission the Royal Society of Chemistry.

Figure 3. SEM images of nanofibrous membranes (a) F(mipB), (b) F(nipB), (c) F(mipT), (d) F(nipT), (e) F(mipBT3), (f) F(nipBT3), (g) F(mipB + mipT), (h) F(nipB + nipT) (32) Reproduced with permission from Elsevier publishers.

Figure 4. (a) Binding of labeled theophylline on theophylline imprinted polymer nanofiber (solid square) and nonimprinted polymer nanofiber (open circle). (b) Binding of labeled estradiol on estradiol imprinted polymer nanofiber (solid square) and non-imprinted polymer nanofiber (open circle) (37) Reproduced with permission from American Chemical Society.

Figure 5. Schematic representation of proximity scintillation process with composite MIP nanofiber material. Bottom left: when ^{3}H-labeled tracer (triangle with star) binds to the MIP nanoparticle, energy from radioactive decay is transferred into optical signal through the adjacent PS-DPA relay system. Top right: in the presence of an excess of non-labeled analyte (open triangle), ^{3}H-labeled analyte is displaced from the binding site and becomes too distant from the nanofiber to achieve effective energy transfer to the PS-DPA system (39) Reproduced with permission from the Royal Society of Chemistry.

Figure 6. (I) The preparation of molecularly imprinted organogel nanofibers. (II) Scanning electron microscopy (SEM) images of (a) a dried gel and (b) molecularly imprinted polymerized organogel (MIPG) nanofibers. The organogelator concentration was 10 wt% in methanol. (III) Amounts of molecules bound by the MIPG and NIPG nanofibers to the theophylline and its structural analogue caffeine and (b) the kinetic binding profile of the MIPG and NIPG nanofibers for the theophylline (44) Reproduced with permission from the Royal Society of Chemistry.

Table 1 Preparation scheme of nanofibers membranes

Nanofiber Membrane	Nanoparticles (g)					
	mipB	**nipB**	**mipT**	**nipT**	**mipBT3**	**nipBT3**
F(mipB)	0.4	0	0	0	0	0
F(nipB)	0	0.4	0	0	0	0
F(mipT)	0	0	0 .4	0	0	0
F(nipT)	0	0	0	0.4	0	0
F(mipBT3)	0	0	0	0	0.4	0
F(nipBT3)	0	0	0	0	0	0.4
F(mipB + mipT)	0.2	0	0.2	0	0	0
F(nipB + nipT)	0	0.2	0	0.2	0	0

F(mip B), F(mipT), F(mipBT3), F(mipB + mipT): nanofibers membranes containing mipB, mipT, mipBT3, mipB and mipT together, respectively.

F(nip B), F(nipT), F(nipBT), F(nipB + nipT): nanofibers membranes containing nipB, nipT, nipBT, nipB and nipT together, respectively. (32) Adapted with permission from Elsevier publishers.